Advances in Aircraft and Spacecraft Science, *Vol. 4, No. 5 (2017) 515-528*
DOI: https://doi.org/10.12989/aas.2017.4.5.515

Delamination evaluation on basalt FRP composite pipe by electrical potential change

Wael A. Altabey*[1,2]

[1]*International Institute for Urban Systems Engineering, Southeast University, Nanjing 210096, China*
[2]*Department of Mechanical Engineering, Faculty of Engineering, Alexandria University, Alexandria 21544, Egypt*

(Received March 2, 2017, Revised April 25, 2017, Accepted April 26, 2017)

Abstract. Since composite structures are widely used in structural engineering, delamination in such structures is an important issue of research. Delamination is one of a principal cause of failure in composites. In This study the electrical potential (EP) technique is applied to detect and locate delamination in basalt fiber reinforced polymer (FRP) laminate composite pipe by using electrical capacitance sensor (ECS). The proposed EP method is able to identify and localize hidden delamination inside composite layers without overlapping with other method data accumulated to achieve an overall identification of the delamination location/size in a composite, with high accuracy, easy and low-cost. Twelve electrodes are mounted on the outer surface of the pipe. Afterwards, the delamination is introduced into between the three layers (0°/90°/0°)s laminates pipe, split into twelve scenarios. The dielectric properties change in basalt FRP pipe is measured before and after delamination occurred using arrays of electrical contacts and the variation in capacitance values, capacitance change and node potential distribution are analyzed. Using these changes in electrical potential due to delamination, a finite element simulation model for delamination location/size detection is generated by ANSYS and MATLAB, which are combined to simulate sensor characteristic. Response surfaces method (RSM) are adopted as a tool for solving inverse problems to estimate delamination location/size from the measured electrical potential changes of all segments between electrodes. The results show good convergence between the finite element model (FEM) and estimated results. Also the results indicate that the proposed method successfully assesses the delamination location/size for basalt FRP laminate composite pipes. The illustrated results are in excellent agreement with the experimental results available in the literature, thus validating the accuracy and reliability of the proposed technique.

Keywords: delamination assessing; electrical capacitance sensor (ECS); basalt FRP pipe; FEM; response surfaces method (RSM); least square error method

1. Introduction

Delamination is a major failure mode in structures manufactured from polymer-matrix composite materials reinforced with fibers as a basalt FRP and has been a subject of intensive research for many years. The delamination detection in general is a difficult and expensive job to

*Corresponding author, Assistant Professor, E-mail: wael.altabey@gmail.com

http://www.techno-press.org/?journal=aas&subpage=7 ISSN: 2287-528X (Print), 2287-5271 (Online)

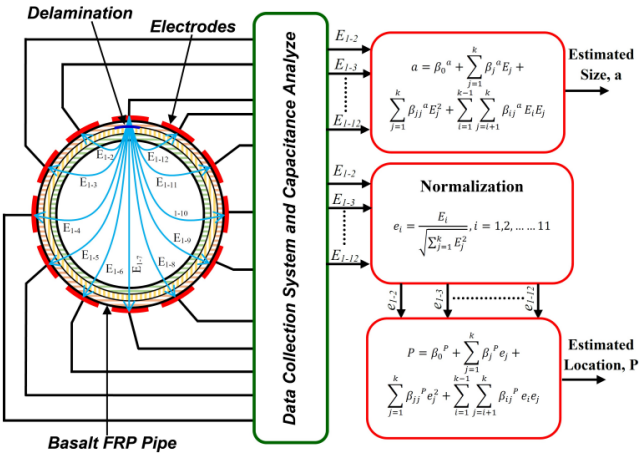

Fig. 1 Sketch of 12-electrode electrical capacitance sensor (ECS) system with response surfaces method

distinguish during inspection. This difficulty of detection indicate to the importance of development of easy and economical technique for monitoring delamination in fiber reinforced polymer (FRP) laminate composites.

Non-destructive testing (NDT) methods have been found to be useful for in-situ evaluation of composites structures, where the structural integrity of laminate composite structures can be assessed effectively.

ECS is one of the most mature and promising NDT methods, which measures the capacitance change of multi-electrode sensor due to the change of dielectric permittivity. It has the characteristics such as low cost, fast response, non-intrusive method, broad application, safety (Yang *et al.* 1995a, 1995b, Li and Huang 2000, Mohamad *et al.* 2012 and Zhang *et al.* 2014). The need for a more accurate measurement of ECS led to the study of the factors which have influence and effect on ECS sensitivity and sensitive domain of ECS electrodes. There are three factors have been studied and found which have effect on ECS measurements, e.g., pipeline material, inner dielectric permittivity (Jaworski and Bolton 2000, Pei and Wang 2009, Al-Tabey 2010, Asencio *et al.* 2015, Sardeshpande *et al.* 2015, Mohamad *et al.* 2016, Altabey 2016) and the ratio of pipeline thickness and diameter (Daoye *et al.* 2009, Altabey 2016), later Altabey (2016) found that the ECS environment temperature is effect on ECS sensitivity and sensitive domain of ECS electrodes with high percentage, so the environment temperature is the fourth factor of factors which have influence on ECS measurement sensitivity.

In this study, in order to identify and localize hidden delamination in basalt FRP laminate composite pipe using electrical potential (EP) technique, a FEM models are generated using ANSYS and MATLAB. Afterwards, the delamination was introduced into between the pipe layers with varying size and location for simulating the dielectric properties change due to delamination and analyzed under each delamination scenario and estimated them using the response surfaces method.

2. Principle of electrical capacitance sensor (ECS)

ECS consists of insulating pipe, measurement electrode, radial screen and earthed screen (Yang

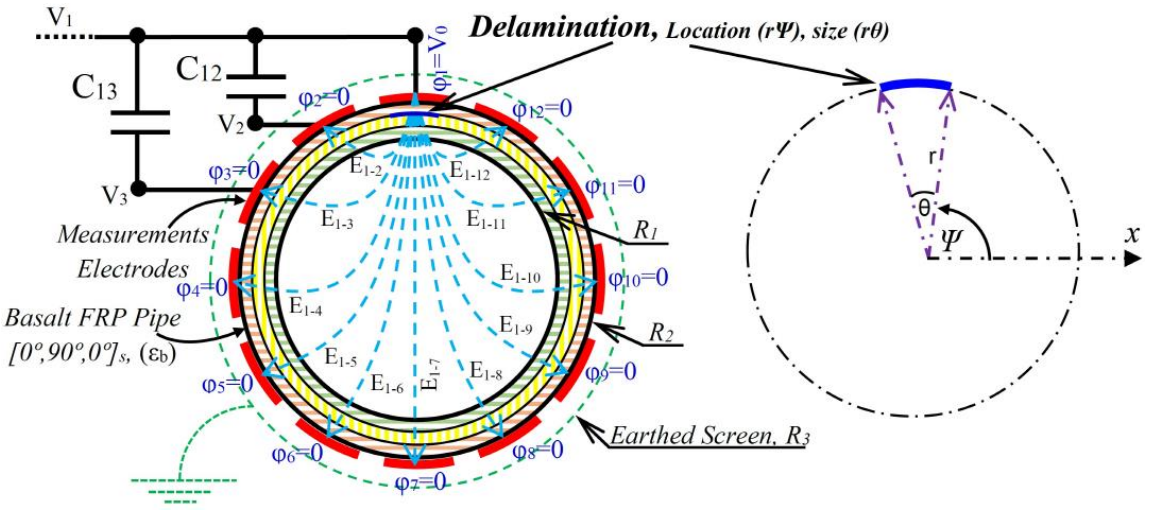

Fig. 2 Schematic representation of the geometrical model and measurement principle of an ECS

and York 1999). The measurement electrode is mounted symmetrically around the circumference of pipeline. Radial screen is fitted between the electrodes to cut the electro-line external to the sensor pipeline and reduce the inter-electrode capacitance. The earthed screen surrounds the measurement electrodes to shield external electromagnetic noise. In most application, ECS electrode is mounted outside the pipeline which is called external electrode ECS (Yang 1997). Electrical capacitance system includes sensor, capacitance measuring circuit and imaging computer is shown in Fig. 1.

2.1 The ECS composition and working principle

For 12-electrode system, the electrodes are numbered as shown in the Fig. 2, are excited with an electric potential, one at a time in increasing order, when one electrode is excited, the other electrodes are kept at ground potential as shown in the Fig. 2 and act as detector electrodes. When electrode No. 1 is excited with a potential, the change $Q_{1,j}$ is induced on the electrodes, j=2,… …., N can be measured.

Next, electrode No. 2 is excited whereas, rest the electrodes are kept at ground potential, and the induced charges Q_{23}, Q_{24}, …, Q_{2N} (N=12) are measured. The measurement protocol continues unit electrode N−1 is excited. Using these charge measurements, the inter electrode capacitance C_{ij} can be computer using the definition of capacitance (Eq. (1)) i.e.,

$$C_{ij} = \frac{Q_{ij}}{\Delta V_{ij}} \tag{1}$$

Where Q_{ij} is the charge induced on electrode j when electrode i is excited with a known potential. V_{ij} is the potential difference between electrodes i and j($\Delta V_{ij}=V_i-V_j$). So the number of independent capacitance measurements M=66 using Eq. (2) is

$$M = \frac{N(N-1)}{2} \tag{2}$$

Table 1 Sensor physical specification

ECS system	Specification
No. of electrodes	8, 12, 16
Space between electrodes	3, 2, 1 mm
Pipe diameter (d_i)	94 mm
Pipe thickness (h)	6 mm
Earth Screen diameter	110 mm
Thickness of electrodes	1 mm
height of electrodes	0.3 m
Permittivity Basalt fiber/Polymer	ε_b = 2.2 Fm^{-1}
Permittivity of Water	ε_w = 80 Fm^{-1}
Permittivity of Air	ε_a = 1.0 Fm^{-1}
Excitation voltage	φ = 15 Volts

Table 2 Physical and mechanical properties of the basalt FRP

E_1	E_2=E_3	G_1=G_3	G_2	υ_1=υ_3	υ_2	ρ
96.74 GPa	22.55 GPa	10.64 GPa	8.73 GPa	0.3	0.6	2700 kg/m^3

3. Finite element simulation model

3.1 ECS System geometrical model

Fig. 2 shows the cross section of 12-electrode ECS system, the sensors physical specifications and the permittivity values of basalt FRE composite pipe are shown in Table 1.

3.2 The basalt FRP pipe material model

Physical and mechanical properties of the basalt FRP laminate composite pipe are shown in Table 2.

3.3 ECS governing equation

In terms of Electrical Capacitance sensor (ECS), the forward problem is the problem of calculating the capacitance matrix C from a given set of sensor design parameters and a given cross-sectional permittivity distribution $\varepsilon(x,y)$.

$$\nabla.\varepsilon(x,y)\nabla\varphi(x,y) = 0 \tag{3}$$

Where $\varphi(x,y)$ is the potential distribution inside the ECS that is determined by solving the Poisson's equation. For the boundary condition imposed on the ECS head by the measurement system. The electric field vector $E(x,y)$, the electric flux density $D(x,y)$ and the potential function $\varphi(x,y)$ are related as follows

$$E(x,y) = -\nabla\varphi(x,y) \tag{4}$$

$$D = \varepsilon(x, y)E(x, y) \tag{5}$$

The change on the electrodes, and hence the inter electrode capacitances can be found using the definition of the capacitance and Gauss's law based on the following surface integral

$$Q_{ij} = \oint_{S_j} (\varepsilon(x, y)\nabla\varphi(x, y).\hat{n})\, ds \tag{6}$$

Where: $\nabla.\varepsilon(x,y)$ is the divergence of permittivity distribution, $\nabla\varphi(x,y)$ is the gradient of potential distribution, S_j is a surface enclosing electrode j, ds is an infinitesimal area on electrode j, $\hat{n}$ is the unit vector normal to S_j and ds is an infinitesimal area on that.

3.4 The FE model description

In this section, the numerical models for simulating the delamination scenarios in basalt FRP pipe will be addressed using ANSYS ver.15. 2D FE software. The approach taken by ANSYS 2D is to divide the different materials and geometries into triangular elements, because many pipes are round under the circumstances of a smaller number of pixels, we can achieve higher accuracy to use the triangular mesh instead of rectangular grids, and then to represent the electric field (see Eq. (4)) within each element with a separate polynomial at six integration points location. For FE simulating of basalt FRP pipe, electrostatic module (PLANE121), triangular 6-node, and the element has one degree of freedom, voltage, at each node. The 6-node elements have compatible voltage shapes and are well suited to model curved boundaries. The total number of mesh elements used for the analysis was 9798 elements.

The potential boundary conditions were applied to the sensor-plate (electrodes). For one electrode, the boundary condition of electric potential ($V=V_0$) with 15V (V_0) was applied and another electrode was kept at ground (V=0) potential to simulate a 15V (RMS) potential gradient across the electrodes. For representing the natural propagation of electric field, the default boundary condition of continuity $(\hat{n}.(D_1 - D_2) = 0)$ was maintained for the internal boundaries.

4. Response surface for the electric potential difference method

The response surface is a widely adopted tool for quality engineering fields (Myers and Montgomery 2002). The response surface methodology brings two advantages, the inverse problems can be approximately solved without consideration of modeling, and the approximated response surfaces can be evaluated using powerful statistical tools. In the present study, the response surface methodology was adopted as a solver for predicting of the delamination locations/sizes from measured electric potential difference, this is one of the inverse problems (see Fig. 1). For most of the response surfaces, the functions for the approximations are polynomials because of simplicity. For the cases of quadratic polynomials, the response surface is described as follow

$$y = \beta_0 + \sum_{j=1}^{k} \beta_j x_j + \sum_{j=1}^{k} \beta_{jj} x_j^2 + \sum_{i=1}^{k-1} \sum_{j=i+1}^{k} \beta_{ij}\, x_i x_j \tag{7}$$

Where k is the number of variables. In the case of 12 electrode type specimens, there are 12 electric potential difference variables; V_0, $E_{1\text{-}2}$, $E_{1\text{-}3}$, ... and $E_{1\text{-}12}$, y is the response surface for estimations of delamination location (Ψ) and size (θ) and the coefficients β are obtained with the least square errors method (Myers and Montgomery 2002, Jiang *et al*. 2014).

To improve the estimation performance of the delamination location/size, the normalizations of the measured electric potential differences are performed. In the case of 12-electrodes, each measured result is normalized by means of the norm of the vector of measured electric potential differences. Each element is divided by the square root sum and replacement the vector ($E_{1\text{-}2}$, $E_{1\text{-}3}$,..., $E_{1\text{-}12}$) in Eq. (7) with norm vector ($e_{1\text{-}2}$, $e_{1\text{-}3}$,…, $e_{1\text{-}12}$). Each element is divided by the square root sum of all results as follows

$$(e_{1-2}, \cdots\cdots\cdots, e_{1-12}) = \left(\frac{E_{1-2}}{\sqrt{{E_{1-2}}^2 + \cdots\cdots + {E_{1-12}}^2}}, \cdots\cdots\cdots, \frac{E_{1-12}}{\sqrt{{E_{1-2}}^2 + \cdots\cdots + {E_{1-12}}^2}} \right) \tag{8}$$

In the case that varies delamination scenarios, the total number of scenarios is n, the response surface can be expressed as follows using matrix expression

$$Y = X\beta + \lambda \tag{9}$$

Where: $Y = \begin{Bmatrix} y_1 \\ y_2 \\ \vdots \\ y_n \end{Bmatrix}$, $X = \begin{bmatrix} 1 & x_{11} & x_{12} & \ldots & x_{1k} \\ 1 & x_{21} & x_{22} & \ldots & x_{2k} \\ \vdots & \vdots & \vdots & \ddots & \vdots \\ 1 & x_{n1} & x_{n2} & \ldots & x_{nk} \end{bmatrix}$, $\beta = \begin{Bmatrix} \beta_0 \\ \beta_1 \\ \vdots \\ \beta_k \end{Bmatrix}$, $\lambda = \begin{Bmatrix} \lambda_1 \\ \lambda_2 \\ \vdots \\ \lambda_n \end{Bmatrix}$

Where λ is an error vector. The unbiased estimator b of the coefficient vector β is obtained using the well-known least square error method as follows

$$b = (X^T X)^{-1} + X^T Y \tag{10}$$

The variance-covariance matrix of the b is obtained as follows

$$Cov(b_i, b_j) = \sigma^2 \, (X^T X)^{-1} \tag{11}$$

Where the σ is the error of Y. The estimated value of σ is obtained as follows

$$\sigma^2 = \frac{SS_E}{n - k - 1} \tag{12}$$

SS_E is a square sum of errors, and expressed as follows

$$SS_E = Y^T Y - b^T X^T Y \tag{13}$$

In order to judge the goodness of the approximation of the response surface, the adjusted coefficient of multiple determination R^2_{adj} is used

$${R^2}_{adj} = 1 - \frac{SS_E/(n - k - 1)}{S_{yy}/(n - 1)} \tag{14}$$

Where S_{yy} is the total sum of squares

Table 3 Convergence study of normalization electrical potential differences of the CFRE laminated composite beams

e_{1-2}	(1)	0.9918	0.2922	0.6931	0	0	0.6315	0.1897	0.0105	0.3158	0.0184
	(2)	0.9914	0.2873	0.6877	0	-0.0057	0.6007	0.1869	0.0059	0.3111	0.0139
e_{2-3}	(1)	0.0015	0.3512	0.7177	0.1683	0	0.3724	0.3711	0.0158	0.4531	0.0187
	(2)	-0.1305	0.3478	0.7127	0.1669	-0.0172	0.3682	0.3686	0.0094	0.4470	0.0139
e_{3-4}	(1)	0	0.4497	0.1380	0.5911	0.5125	0.5848	0.7355	0.0008	0.3992	0
	(2)	0	0.4461	0.1375	0.5881	0.5113	0.5813	0.7294	0	0.3976	0
e_{4-5}	(1)	0	0.5243	0.0173	0.6786	0.7826	0.4106	0.5473	0	0.5481	0.2392
	(2)	0	0.5217	0.0125	0.6754	0.7814	0.4069	0.5451	0	0.5457	0.2371
e_{5-6}	(1)	0	0.3269	0	0.3721	0.2894	0.0006	0	0.5900	0.4711	0.2671
	(2)	0	0.3251	-0.0125	0.3698	0.2873	0	0	0.5885	0.4692	0.2650
e_{6-7}	(1)	0	0.4699	0	0.1856	0.2175	0	0	0.8111	0.1683	0.9369
	(2)	0	0.4687	0	0.1823	0.2126	0.0065	-0.0026	0.8085	0.1655	0.9344
Location	(1)	127.35	-113.23	-81.53	-68.37	-18.22	7.86	19.58	67.34	97.39	108.19
	(2)	-127.5	-113.5	-82	-69	-18.5	8	20	68	98	109
Size	(1)	5.48	4.87	1.96	5.46	5.92	2.91	5.96	8.48	5.98	4.95
	(2)	5.5	5	2	5.5	6	3	6	8.5	6	5

(1) Proposed method, (2) Todoroki *et al.* (2004)

$$S_{yy} = Y^T Y - \frac{(\sum_{i=1}^{n} y_i)^2}{n} \tag{15}$$

The value of R^2_{adj} is equal to or lower than 1.0. A higher value of R^2_{adj} implies a better fit. When the response surface shows a very good fit, R^2_{adj} approaches 1.0. A good fit of the response surface means that the response surface gives good estimations for the electrical potential (EP) technique used for the regression. Lower R^2_{adj} values means poorer estimations and the error band of the estimated result is wider.

5. Results and discussions

5.1 Convergence study and accuracy

In this subsection, a convergence investigation is carried out for the proposed method, the normalization electrical potential differences between electrodes due to delamination are calculated and compared with available experimental results in literatures. The dataset used for validation of presented technique is adapted from Todoroki *et al.* (2004). The tests were conducted on composite laminated beams were manufactured from unidirectional layers of carbon/epoxy (CFRE), the stacking sequence is $(0_2/90_2)_s$ and the thickness of the laminates is approximately t=1 mm. The fiber volume fraction is approximately V_f=0.5. The beam type specimens have the length of 270 mm and the width of 15 mm. Seven electrodes are mounted on the specimen surface. All of these electrodes are placed on a single side of a specimen. For electrode model, the thickness of

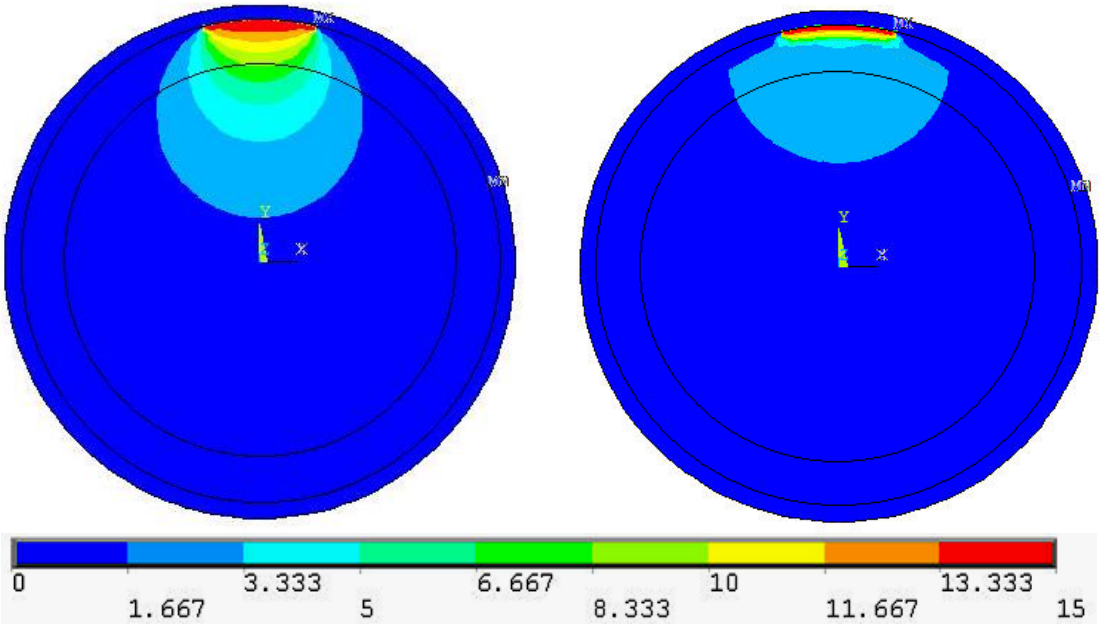

Fig. 3 The node potential distribution of basalt FRP laminated composite pipe before embedded delamination right and after embedded delamination left

electrodes is 10 mm, the space between electrodes is 45 mm and the boundary condition of electric potential ($V=V_0$) with +5V (V_0). The electrical potential changes of each segment between electrodes are measured for various cases of location and size of delaminations. From the measured data, the relationships between electrical potential change and location and the size of the delaminations are obtained using response surface method. Table 3 presents a convergence and comparison study for the proposed method data and the experimental data of Todoroki *et al.* (2004).

From Table 3 it can be observed that the numerical results are in an excellent agreement with experimental results of normalization electrical potential differences presented by Todoroki *et al.* (2004). This validates the precision of the presented technique.

5.2 Electrical potential differences method for delamination assessing

To investigate the effect of the delamination on the dielectric properties in basalt FRP pipe, the FE analysis of the electric field intensity of basalt FRP piping system were performed using commercially available 2D FE software, ANSYS (The Electrostatic Module in the Electromagnetic subsection of ANSYS (2015), Al-Tabey (2012). The software only computes the potential and the electric field values at the element nodes and interpolate between these nodes to obtain the values for other points within the elements.

The Simulations, and node potential distribution of pressurized basalt FRP laminated composite pipe before and after delamination occurred for the ANSYS 2D simulation, when electrode (1) is excited are illustrated in Fig. 3 right and left respectively.

The blue area represents the region of the pipe without potential i.e., $\varphi=0$ but the colored areas represent the region of the pipe having the different potential (different node potential) i.e., the

Table 4 Numerical results of electric potential differences for each delamination scenario (Del_i)

Delamination Scenario (degree)			Electric potential difference (V)											
Del_i	Ψ°	θ°	E_{1-1}	E_{1-2}	E_{1-3}	E_{1-4}	E_{1-5}	E_{1-6}	E_{1-7}	E_{1-8}	E_{1-9}	E_{1-10}	E_{1-11}	E_{1-12}
Del_0	Non		15	7.5	4.93	4.03	3.7	3.57	3.57	3.57	3.7	4.03	4.93	7.5
Del_1	0	5	15	7.5	4.93	4.03	3.7	3.57	3.57	3.57	3.7	3.33	4.93	7.5
Del_2	30	6.75	15	7.5	4.93	4.03	3.7	3.57	3.57	3.57	3.7	4.03	4.11	7.5
Del_3	60	8.5	15	7.5	4.93	4.03	3.7	3.57	3.57	3.57	3.7	4.03	4.93	7.15
Del_4	90	10	15	7.2	4.3	3.82	3.53	3.33	2.5	3.33	3.53	3.82	4.3	7.2
Del_5	120	11.75	15	6.98	4.93	4.03	3.7	3.57	3.57	3.57	3.7	4.03	4.93	7.5
Del_6	150	13.5	15	7.5	4	4.03	3.7	3.57	3.57	3.57	3.7	4.03	4.93	7.5
Del_7	180	15	15	7.5	4.93	3.33	3.7	3.57	3.57	3.57	3.7	4.03	4.93	7.5
Del_8	210	16.75	15	7.5	4.93	4.03	3.42	3.57	3.57	3.57	3.7	4.03	4.93	7.5
Del_9	240	18.5	15	7.5	4.93	4.03	3.7	3.12	3.57	3.57	3.7	4.03	4.93	7.5
Del_{10}	270	20	15	7.5	4.93	4.03	3.7	3.57	3	3.57	3.7	4.03	4.93	7.5
Del_{11}	300	21.75	15	7.5	4.93	4.03	3.7	3.57	3.57	2.86	3.7	4.03	4.93	7.5
Del_{12}	330	23.5	15	7.5	4.93	4.03	3.7	3.57	3.57	3.57	3.33	4.03	4.93	7.5

domain of electrode can be sensitive or detection domain.

From the Simulation Fig. 3, we can notice that the significant difference before and after introduced delamination in the node potential and electric field intensity.

The capacitance values between electrodes (C_{ij}) and potential differences (E_{ij}) from 2D simulations are calculated before (Del_0) and after (Del_i) delamination, where i=1, 2 …. is the number of delamination scenarios (FE models). In this study must be used at least twelve delamination scenarios of delamination location/size for validating the accuracy and reliability of the proposed technique. To study the behavior of ECS working under varying the delamination location/size, we are selected four various scenarios of delamination location/size in basalt FRP laminate composite pipe, the first scenario (Del_1) has size θ=5º, is located at r=51 mm and Ψ=0º, the second scenario (Del_4) has size θ=10º, is located at r=51 mm and Ψ=90º, the third delamination scenario (Del_7) has size θ=15º, is located at r=51 mm and Ψ=180º and final scenario (Del_{10}) has size θ=20º, is located at r=51 mm and Ψ=270º, respectively, as shown in Table 4.

Using the scripting capabilities in ANSYS we can simulate capacitance values (C_{ij}) and potential differences (E_{ij}) between electrodes, before (Del_0) and after (Del_i) introduced delamination.

The 66 capacitance measurements (C_{ij}) for each delamination scenarios in composite pipe are illustrated together in Fig. 4. As shown in the Fig. 4, we can see that the effect of the delamination occurred on the capacitance measurements (C_{ij}) distributions the degradation in capacitance values between electrodes is occurred, this degradation is depend on the delamination size (θ), as increases of the delamination size (θ), the capacitance values decreased.

The electrical potential differences (E_{ij}) when electrode (1) is excited for four delamination scenarios in composite pipe are illustrated together in Fig. 5. As shown in the Fig. 5 and Table 4, we can see that the effect of the delamination on the node potential distributions, the degradation in potential differences is occurred, but only in the values of the potential differences according to the electrode that mounted close to the location of delamination occurred (e.g., the degradation in

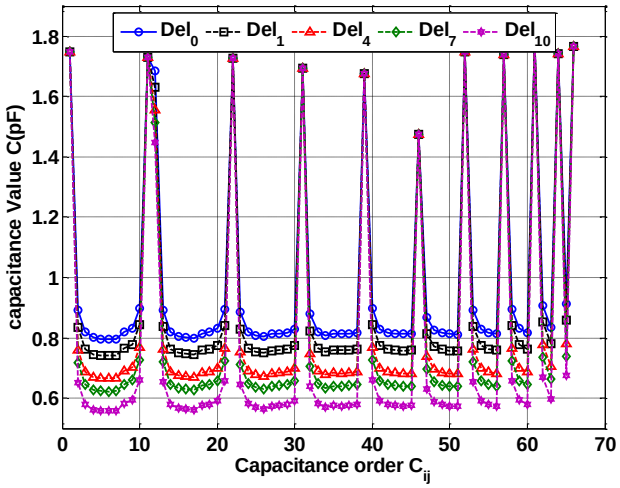

Fig. 4 Effect of delamination scenarios (Del_i) on capacitance values between electrodes (pF)

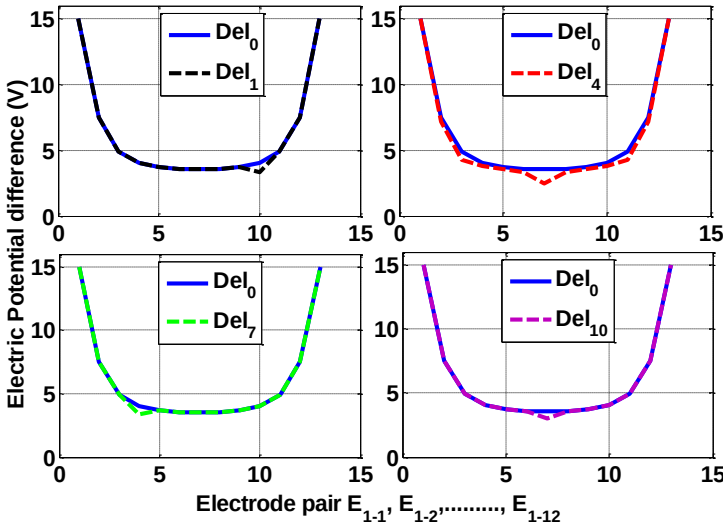

Fig. 5 Effect of delamination scenarios change on electric potential difference (V) when electrode (1) is excited

$E_{1\text{-}4}$ value is due to delamination scenario (Del_7), $E_{1\text{-}7}$ value is due to scenario (Del_{10}) and $E_{1\text{-}10}$ value is due to scenario (Del_1)) except delamination scenario (Del_4) is influenced on the all potential differences values from $E_{1\text{-}2}$ to $E_{1\text{-}12}$, because, the delamination is located close to the excited electrode (1), and so on this behavior will be repeated when the other electrodes are excite (see Fig. 2).

Fig. 6 shows the sensor sensitivity versus delamination scenarios (Del_i). The sensor sensitivity is defined as

$$Sensor\ sensitivity\% = \frac{C_{\mathrm{del}_0} - C_{\mathrm{del}_i}}{C_{\mathrm{del}_0}} \times 100 \tag{16}$$

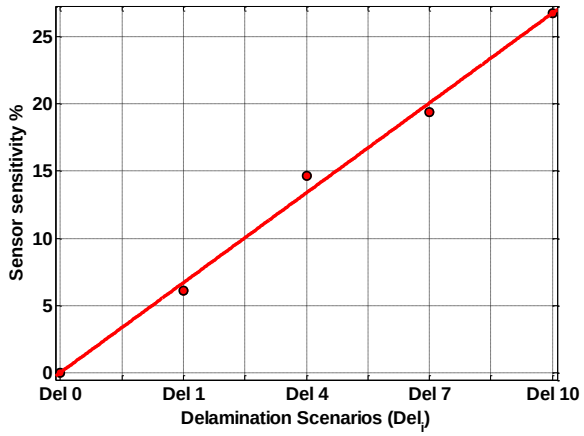

Fig. 6 Capacitance sensor sensitivity versus delamination scenarios (Del_i)

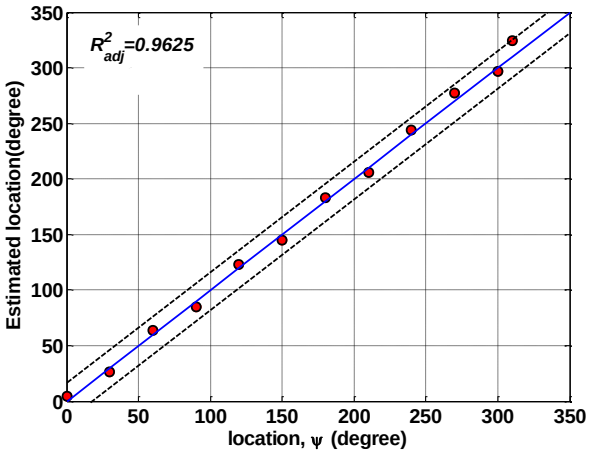

Fig. 7 Estimation results of delamination Location, Ψ in basalt FRP laminate composite pipe

Where: C_{delo} and C_{deli} are the capacitance measurements for before and after delamination occurred respectively. The sensor sensitivity is dependent on the delamination size (θ), as increase of the delamination size (θ), the sensor sensitivity increases, the sensor has a sensitivity ranging between 6.13% and 26.723% for scenario (Del_1) to scenario (Del_{10}) respectively and selected sensor geometrical parameters.

5.3 Estimation of delamination location/size

Figs. 7 and 8 show the estimated results of the delamination location, Ψ and size, θ in basalt FRP laminate composite pipe of response surface method. The R^2_{adj} of these results are 0.9625 and 0.9357 for location and size respectively. All of the estimations are plotted on the diagonal line. The error band is defined as the maximum error of the estimated location and size. The error band from the diagonal line is less than 8 degrees and 2.5 degrees for estimated location and size, respectively. The results of the estimated location and size due to electric potential difference between electrodes from ECS (see Table 4) is presented in Table 5. As a result, the response

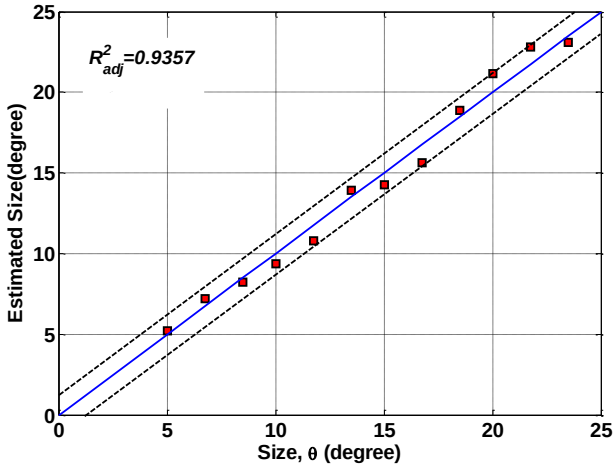

Fig. 8 Estimation results of delamination size, θ in basalt FRP laminate composite pipe

Table 5 Estimations and errors of response surfaces method data (unit degree)

Delamination Scenario		Estimated Delamination		Error of Estimations	
Size, θ	Location, Ψ	Size, θ	Location, Ψ	Size, θ	Location, Ψ
5	0	5.23	4.215	0.23	4.215
6.75	30	7.22	26.3	0.47	3.7
8.5	60	8.21	63.5	0.29	3.5
10	90	9.38	85.22	0.62	4.78
11.75	120	10.77	122.9	0.98	2.9
13.5	150	13.9	144.87	0.4	5.13
15	180	14.256	183.52	0.744	3.52
16.75	210	15.64	206.21	1.11	3.79
18.5	240	18.85	244.23	0.35	4.23
20	270	21.16	277.3	1.16	7.3
21.75	300	22.8	296.8	1.05	3.2
23.5	330	23.12	324.64	0.38	5.36

surfaces gave good estimations for FE data even to identify and localize delamination in basalt FRP laminate composite pipe.

6. Conclusions

In the present work, the delamination identifications of the location and size in basalt fiber reinforced polymer (FRP) laminated composite pipe are performed using the electrical potential (EP) technique with response surfaces method. The illustrated results are in excellent agreement with the experimental results available in the literature, thus validating the accuracy and reliability of the proposed technique and the following conclusions can be drawn:

1. Electric potential difference due to delamination creation can be measured with multiple

electrodes mounted on an outer surface in a basalt FRP pipe.

2. The delamination size variation was found an influence on the sensor sensitivity and identification performance.

3. Delamination size identifications with response surfaces can be successfully performed for twelve scenarios of delamination size in basalt FRP laminates pipe with adjusted coefficient of multiple determination R^2_{adj} is 0. 0.9357.

4. Delamination location identifications with response surfaces can be successfully performed for twelve scenarios of delamination location in basalt FRP laminates pipe with adjusted coefficient of multiple determination R^2_{adj} is 0.9625.

5. The response surfaces method gave good estimations for FEM data even for extrapolations within the error band of less than 8 and 2.5 degrees for delamination location and size respectively.

6. Finally, the proposed method successfully provides delamination assessing for a basalt FRP laminate composite pipe including the delamination location/size investigation.

References

Al-Tabey, W.A. (2010), "Effect of pipeline filling material on electrical capacitance tomography", *Proceedings of the International Postgraduate Conference on Engineering (IPCE 2010)*, Perlis, Malaysia, October.

Al-Tabey, W.A. (2012), *Finite Element Analysis in Mechanical Design Using ANSYS: Finite Element Analysis (FEA) Hand Book For Mechanical Engineers With ANSYS Tutorials*, LAP Lambert Academic Publishing, Germany.

Altabey, W.A. (2016), "Detecting and predicting the crude oil type inside composite pipes using ECS and ANN", *J. Struct. Monitor. Mainten.*, **3**(4), 377-393.

Altabey, W.A. (2016), "FE and ANN model of ECS to simulate the pipelines suffer from internal corrosion", *J. Struct. Monitor. Mainten.*, **3**(3), 297-314.

Altabey, W.A. (2016), "The thermal effect on electrical capacitance sensor for two-phase flow monitoring", *J. Struct. Monitor. Mainten.*, **3**(4), 335-347.

ANSYS Low-Frequency Electromagnetic analysis Guide, The Electrostatic Module in the Electromagnetic subsection of ANSYS (2015), ANSYS, Inc. Southpointe 275 Technology Drive Canonsburg, PA 15317, U.S.A.

Asencio, K., Bramer-Escamilla, W., Gutiérrez, G. and Sánchez, I. (2015), "Electrical capacitance sensor array to measure density profiles of a vibrated granular bed", *J. Powd. Technol.*, **270**, 10-19.

Daoye, Y., Bin, Z., Chuanlong, X., Guanghua, T. and Shimin, W. (2009), "Effect of pipeline thickness on electrical capacitance tomography", *Proceedings of the 6th International Symposium on Measurement Techniques for Multiphase Flows, J. Phys.: Conf. Ser.*, **147**, 1-13.

Jaworski, A.J. and Bolton, G.T. (2000), "The design of an electrical capacitance tomography sensor for use with media of high dielectric permittivity", *Measure. Sci. Technol.*, **11**(6), 743-757.

Jiang, S., Li, D., Zhou, C. and Zhang, L. (2014), "Capabilities of stochastic response surface method and response surface method in reliability analysis", *Struct. Eng. Mech.*, **49**(1), 111-128.

Li, H. and Huang, Z. (2000), *Special Measurement Technology and Application*, Zhejiang University Press, Hangzhou, China.

Mohamad, E.J., Rahim, R.A., Leow, P.L., Fazalul, Rahiman, M.H., Marwah, O.M.F., Nor Ayob, N.M., Rahim, H.A. and Mohd Yunus, F.R. (2012), "An introduction of two differential excitation potentials technique in electrical capacitance tomography", *J. Sensor. Actuat. A*, **180**, 1-10.

Mohamad, E.J., Rahim, R.A., Rahiman, M.H.F., Ameran, H.L.M., Muji, S.Z.M. and Marwah, O.M.F. (2016), "Measurement and analysis of water/oil multiphase flow using electrical capacitance tomography sensor", *J. Flow Measure. Instrument.*, **47**, 62-70.

Myers, R. and Montgomery, D.C. (2002), *Response Surface Methodology Process and Product Optimization Using Designed Experiments*, 2nd Edition, Wiley-Interscience, New York, U.S.A.

Pei, T. and Wang, W. (2009), "Simulation analysis of sensitivity for electrical capacitance tomography", *Proceedings of the 9th International Conference on Electronic Measurement & Instruments*.

Sardeshpande, M.V., Harinarayan, S. and Ranade, V.V. (2015), "Void fraction measurement using electrical capacitance tomography and high speed photography", *J. Chem. Eng. Res. Des.*, **9**(4), 1-11.

Todoroki, A., Tanaka, Y. and Shimamura, Y. (2004), "Multi-prove electric potential change method for delamination monitoring of graphite/epoxy composite plates using normalized response surfaces", *J. Compos. Sci. Technol.*, **64**, 749-758.

Yang, W.Q., Stott, A.L., Beck, M.S. and Xie, C.G. (1995a), "Development of capacitance tomographic imaging systems for oil pipeline measurements", *Rev. Sci. Instr.*, **66**(8), 4326.

Yang, W.Q., Beck, M.S. and Byars, M., (1995b), "Electrical capacitance tomography-from design to applications", *Measure. Contr.*, **28**(9), 261-266.

Yang, W.Q. and York, T.A. (1999), "New AC-based capacitance tomography system", *IEEE Proc.: Measure. Sci. Technol.*, **146**(1), 47-53.

Yang, W.Q. (1997), "Modelling of capacitance sensor", *IEEE Proc.: Measure. Sci. Technol.*, **144**(5), 203-208.

Zhang, W., Wang, C., Yang, W. and Wang C. (2014), "Application of electrical capacitance tomography in particulate process measurement-a review", *J. Adv. Powd. Technol.*, **25**, 174-188.

EC